

Detection of 1*H*-Triphosphirene (*c*-HP₃) and 2-Triphosphenylidene (HP₃): The Isovalent Counterparts of 1*H*-Triazirine (*c*-HN₃) and Hydrazoic Acid (HN₃)

Chaojiang Zhang, Cheng Zhu, André K. Eckhardt,* and Ralf I. Kaiser*



Cite This: *J. Phys. Chem. Lett.* 2022, 13, 2725–2730



Read Online

ACCESS |



Metrics & More

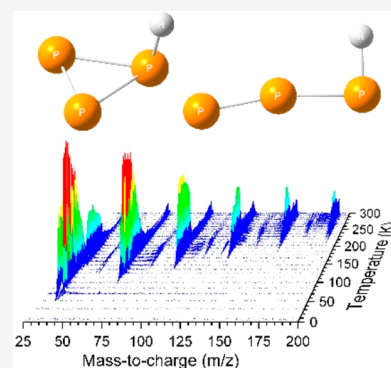


Article Recommendations



Supporting Information

ABSTRACT: The hitherto elusive 1*H*-triphosphirene (*c*-HP₃) and 2-triphosphenylidene (HP₃) molecules were prepared in low-temperature matrices and detected isomer selectively through photoionization coupled with reflectron time-of-flight mass spectrometry (PI-ReTOF-MS). Our results reveal a thermodynamically preferred cyclic isomer (*c*-HP₃) compared to the acyclic structure (HP₃) in contrast to the isovalent HN₃ system favoring hydrazoic acid (HN₃) compared to 1*H*-triazirine (*c*-HN₃). Theoretical computations suggest a ring strain energy of 1*H*-triphosphirene (*c*-HP₃) of only 35 kJ mol⁻¹, which is significantly lower than the tetrahedral phosphorus molecule (P₄) of 74 kJ mol⁻¹. This work provides a fundamental benchmark to understand the electronic structure and chemical bonding of cyclic molecules and offers an unconventional approach to preparing highly strained, still elusive molecules such as 1*H*-triazirine and tetrahedral tetranitrogen (N₄) in the near future involving progressive nonequilibrium chemistries.



Since the first report by Curtius in 1890,^{1,2} hydrazoic acid (HN₃, **1**, Figure 1), the simplest covalent azide, has received extensive attention from the synthetic (in)organic,^{3,4}

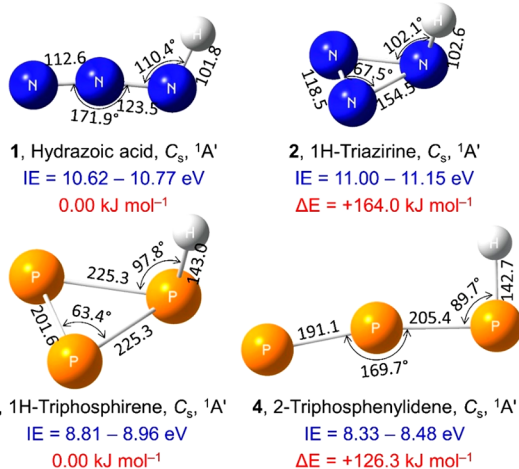


Figure 1. Molecular structures of HN₃ and HP₃ isomers. Bond lengths are given in picometers (pm) and bond angles in degrees; point groups, electronic ground states, computed adiabatic ionization energies corrected for the electric field effect (blue), and relative energies (red) are also shown. The energies were computed at the CCSD(T)/CBS//B3LYP/cc-pVTZ plus zero-point vibrational energies level of theory. The atoms are color coded in white (hydrogen), blue (nitrogen), and orange (phosphorus). Coordinates and normal modes are provided in Tables S5 and S6.

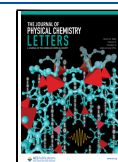
combustion chemistry,^{5,6} physical chemistry,^{7,8} and theoretical chemistry⁹ communities due to its high detonation energy and potential application of liquid energy density materials.^{10,11} Photodissociation experiments of hydrazoic acid at wavelengths shorter than 220 nm found that the cyclic isomer—1*H*-triazirine (*c*-HN₃, **2**, Figure 1)—as a potential reaction intermediate to the *cyclic*-trinitrogen (*c*-N₃) radical.^{12,13} This molecule, which has been inferred as a transient radical in the reaction between nitrous acid (HNO₂) and protonated hydrazine (N₂H₅⁺),^{14,15} represents a benchmark of a strained cyclic compound with a ring strain energy of 198 kJ mol⁻¹.¹⁶ Theoretical computations predicted that 1*H*-triazirine (*c*-HN₃, **2**) is kinetically stable but thermodynamically less favorable by 158 kJ mol⁻¹ with respect to hydrazoic acid (HN₃, **1**). The ring strain energy results in an energy release of up to 20 kJ g⁻¹, which is 1 order of magnitude higher than 2.18 kJ g⁻¹ for trinitrotoluene (TNT).^{17,18} However, 1*H*-triazirine (*c*-HN₃, **2**) has remained elusive to date due to the inherent difficulty in the synthesis and isolation of highly strained and explosive molecules.

In conjunction with Langmuir's concept of isovalency,¹⁹ in which molecular entities with the same number of valence

Received: March 2, 2022

Accepted: March 18, 2022

Published: March 21, 2022



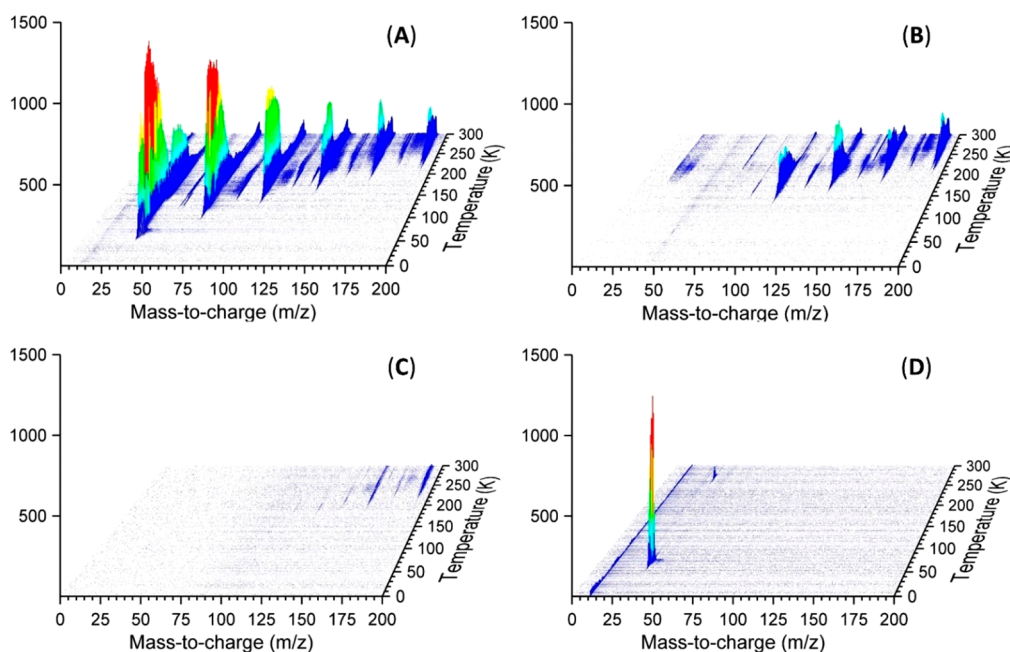


Figure 2. Temperature-dependent mass spectra of the subliming phosphine–dinitrogen ices. The data were recorded at photon energies of (A) 10.49 eV, (B) 8.53 eV, (C) 8.20 eV, and (D) 10.49 eV (blank).

electrons are predicted to have similar chemistries and structures, particular attention has been devoted to the preparation of the isovalent counterparts of hydrazoic acid (HN_3 , **1**) and *1H*-triazirine (*c*- HN_3 , **2**), in which all three nitrogen atoms (N) are replaced by isovalent phosphorus (P) atoms: *1H*-triphosphirene (*c*- HP_3 , **3**)^{20,21} and 2-triphosphenylidene (HP_3 , **4**, Figure 1). *1H*-Triphosphirene (*c*- HP_3 , **3**) has a ring strain energy of only 35 kJ mol⁻¹, which is significantly lower compared to *1H*-triazirine (*c*- HN_3 , **2**) of 198 kJ mol⁻¹¹⁶ and the tetrahedral phosphorus molecule (P_4) of 74 kJ mol⁻¹. This indicates that *1H*-triphosphirene (*c*- HP_3 , **3**) should be easier to prepare than its isovalent *1H*-triazirine (*c*- HN_3 , **2**) counterpart. However, although white phosphorus (P_4) can be transformed into the *cyclo*- P_3 ligand in the process of generating nickel(II) complexes,^{22,23} the preparation of *1H*-triphosphirene (*c*- HP_3 , **3**) has remained a fundamental synthetic challenge due to the lack of preparative synthetic chemistry routes to isolate the *cyclo*- P_3 as σ -donor ligand. Consequently, *1H*-triphosphirene (*c*- HP_3 , **3**) along with its acyclic 2-triphosphenylidene (HP_3 , **4**) isomer exemplifies one of the least explored classes of inorganic molecules.

Here, we report the first preparation of *1H*-triphosphirene (*c*- HP_3 , **3**) together with the 2-triphosphenylidene (HP_3 , **4**) isomer in cryogenic phosphine (PH_3)–dinitrogen (N_2) matrices exposed to energetic electrons at 5 K. Combined with electronic structure calculations, both isomers are unambiguously identified upon the temperature-programmed desorption (TPD) phase of the irradiated ices. This is achieved through *isomer-selective* photoionization in the gas phase accounting for the computed adiabatic ionization energies (IEs) of **3** and **4** (Figure 1) by taking advantage of vacuum-ultraviolet (VUV) photoionization reflectron time-of-flight mass spectrometry (PI-ReTOF-MS). Electronic structure calculations disclose that *1H*-triphosphirene (*c*- HP_3 , **3**) and 2-triphosphenylidene (HP_3 , **4**) can be prepared through decomposition of two triphosphirane (*c*- P_3H_3 , **5**, Figure S3) and 1-triphosphene (P_3H_3 , **6**, Figure S3) transients,

respectively, via molecular dihydrogen loss. The very first preparation and detection of *1H*-triphosphirene (*c*- HP_3 , **3**) and 2-triphosphenylidene (HP_3 , **4**) document their gas-phase stability over at least $10 \pm 1 \mu\text{s}$. These findings not only revolutionize our fundamental knowledge on the chemical bonding and electronic structure of the strained, cyclic group XV molecule *1H*-triphosphirene (*c*- HP_3 , **3**) along with its acyclic isomer 2-triphosphenylidene (HP_3 , **4**) but also afford an unconventional approach to prepare highly strained, still elusive molecules such as *1H*-triazirine (*c*- HN_3 , **2**) and possibly tetrahedral tetranitrogen (N_4) in the near future involving progressive nonequilibrium chemistries.

Fourier-transform infrared spectroscopy (FTIR) was applied to monitor the chemical evolution of the ices during the radiation exposure at 5.0 ± 0.1 K. The absorptions of phosphine were identified in the spectrum of the pristine ice with prominent fundamentals visible at, e.g., 2314 cm⁻¹ (ν_3), 1097 cm⁻¹ (ν_4), and 983 cm⁻¹ (ν_2).²⁴ The irradiation process produced two shoulders at 2270 and 1063 cm⁻¹ and a distinct absorption at 788 cm⁻¹, which are associated with P–H stretching modes, PH_2 scissoring modes, and the deformation mode of phosphorus (P) and nitrogen (N) containing rings,²⁵ respectively. The substitution of N_2 by ¹⁵ N_2 shifted the 788 cm⁻¹ peak to 784 cm⁻¹; this suggests that the structural moiety associated with this absorption contains nitrogen (Table S4). However, since energetic electron irradiation can produce a wide inventory of new species, whose absorptions of the functional groups often overlap in the infrared regime,^{26,27} infrared spectroscopy can determine newly formed *functional groups* but does not always allow identification of *individual molecules* in the case of complex mixtures. Therefore, an alternative method is required to probe discrete isomers selectively.

This is accomplished by photoionizing the subliming molecules in the temperature-programmed desorption (TPD) phase by tunable vacuum-ultraviolet (VUV) photoionization and detecting the ions in a reflectron time-of-flight

mass spectrometer (PI-ReTOF-MS) based on their arrival times on a multichannel plate. By tuning the photoionization energies (PEs)²⁸ above or below the isomer(s) of interest, specific isomers can be selectively ionized and hence identified based on their IEs (Figure 1). Considering the computed IEs of 1*H*-triphosphirene (*c*-HP₃, 3) and 2-triphosphenylidene (HP₃, 4) of 8.81–8.96 and 8.33–8.48 eV, respectively, three PEs of 10.49, 8.53, and 8.20 eV are required. Photons at 10.49 eV can ionize both isomers 3 and 4; 8.53 eV photons can ionize only 4, whereas 8.20 eV photons ionize neither 3 nor 4. The temperature-dependent mass spectra collected at distinct photon energies along with the blank experiment are compiled in Figure 2, whereas the corresponding TPD profiles of the ionized target molecules at mass-to-charge ratios equal to 94 ($m/z = 94$, HP₃⁺) are visualized in Figure 3. At a photon

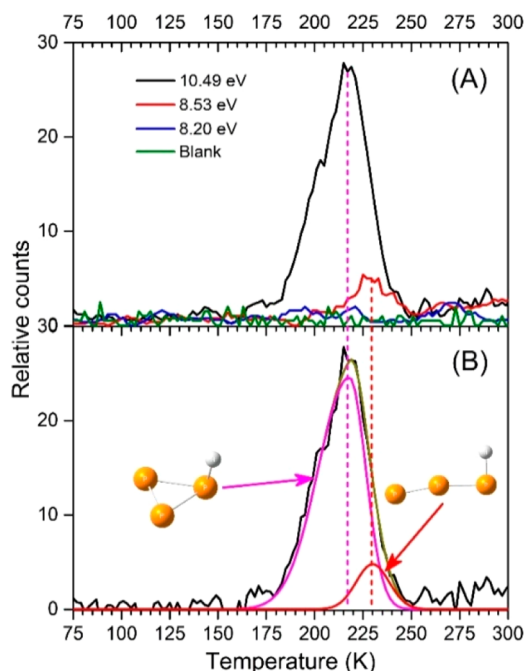


Figure 3. PI-ReTOF-MS profiles at $m/z = 94$ during the TPD phase of the processed phosphine–dinitrogen ices at photon energies of 10.49 eV (black, the line of P₃H is obtained by subtracting the signals above 240 K of $m/z = 94$, Figure S2), 8.53 eV (red), 8.20 eV (blue), and blank, 10.49 eV (green) (A), and the deconvolution of distinct isomers at 10.49 eV (B), in which black line shows the PI-ReTOF-MS signals at $m/z = 94$ extracted the data of blank experiments (green line in (A)).

energy of 10.49 eV (Figure 3A, black line; Figure S1), a broad sublimation event extending from 185 to 250 K can be observed in the TPD profile at $m/z = 94$; this profile has a maximum at 215 K. A control experiment replacing dinitrogen by 15-dinitrogen in the ices reveals no mass shift of this TPD profile (Figure S1), demonstrating that the carrier of the signal at $m/z = 94$ does not contain a nitrogen atom and, hence, can only be assigned to a molecule with the molecular formula HP₃. When the photon energy was lowered to 8.53 eV, a photon energy that only allows 4 to be ionized, the sublimation profile changed significantly. Here, the TPD profile revealed low ion counts from 210 to 250 K peaking at 229 K (Figure 3A, red line). Tuning the photon energy even lower to 8.20 eV, no sublimation event was found at $m/z = 94$ (Figure 3A, blue line). This reveals that the sublimation event with 8.53 eV

photons can be associated with isomer 4, which cannot be ionized at a photon energy of 8.20 eV. Deconvolution of the TPD profile with a bimodal Gaussian functional (Figure 3B)^{29–31} reveals the integrated ratio of the ion counts for both sublimation events at 215 and 229 K to be $(7.4 \pm 0.1):1$ at a photon energy of 10.49 eV. These findings provide compelling evidence for the formation and detection of both 1*H*-triphosphirene (*c*-HP₃, 3) and 2-triphosphenylidene (HP₃, 4). It is critical to highlight that control experiments were also conducted in a fashion similar to that of the actual experiments, but without exposing the ices to energetic electrons in the TPD phase. No ion counts were observed at the $m/z = 94$ (Figure 3A, green line), revealing that the observed ion counts are linked to the energetic processing of the ice mixtures but not the result of potential ion–molecule chemistries in the subliming ices.

Having identified isomers 1*H*-triphosphirene (*c*-HP₃, 3) together with the 2-triphosphenylidene (HP₃, 4), we shift our attention to exploring possible formation pathways. Experiments performed with pure phosphine ices in the same experimental setup under identical experimental conditions prepared neither 3 nor 4.²⁴ However, both studies detected ion counts at $m/z = 96$ (P₃H₃⁺), which can be linked to the triphosphirane (*c*-P₃H₃, 5) and 1-triphosphene (P₃H₃, 6) molecules.²⁴ Decomposition of these isomers via molecular dihydrogen loss could in principle lead via dehydrogenation to 1*H*-triphosphirene (*c*-HP₃, 3) together with the 2-triphosphenylidene (HP₃, 4). These reaction pathways are also supported by electronic structure calculations (Figure 4). Triphosphirane (*c*-P₃H₃, 5) and 1-triphosphene (P₃H₃, 6) exist in two conformers, namely *syn* and *anti* with the *anti* conformers as the energetically preferred form (Figure S3). All conformers are connected through five transition states located between 274.7 and 365.5 kJ mol^{−1} above the reactant to 1*H*-triphosphirene (*c*-HP₃, 3) and 2-triphosphenylidene (HP₃, 4), respectively (Figure 4). The transition state can be overcome through the transfer of kinetic energy from the impinging electrons to triphosphirane (*c*-P₃H₃, 5) and 1-triphosphene (P₃H₃, 6). This one-step molecular hydrogen loss pathway could be also replaced through two successive atomic hydrogen losses yielding eventually also 1*H*-triphosphirene (*c*-HP₃, 3) and 2-triphosphenylidene (HP₃, 4). In the present experiments, the nitrogen molecules within the matrix represent an unconventional oxidizing agent being reduced to hydrazine (N₂H₄); the formation of hydrazine (N₂H₄) is evident from the detection of $m/z = 32$ (N₂H₄) in the TPD phase of the experiments. Therefore, one of the fundamental differences of the phosphine²⁴ and phosphine–dinitrogen systems is the capability of molecular nitrogen to remove hydrogen via four successive addition steps³² eventually forming hydrazine (N₂H₄); this “hydrogen depleted” system supports the formation of 1*H*-triphosphirene (*c*-HP₃, 3) together with 2-triphosphenylidene (HP₃, 4), which were not detected in pure phosphine ices due to the “hydrogen-rich” environments in these matrices.²⁴

We are discussing now the geometric structures and chemical bonding of the newly detected 1*H*-triphosphirene (*c*-HP₃, 3) and 2-triphosphenylidene (HP₃, 4) isomers and comparing these to the isovalent to hydrazoic acid (HN₃, 1) and 1*H*-triazirine (*c*-HN₃, 2). The 1*H*-triphosphirene molecule has a C₃ point group and a ¹A' electronic state (Figure 1). At the B3LYP/cc-pVTZ level of theory, the P–P bond lengths are computed to be 225.3 and 201.6 pm, and the P–H bond

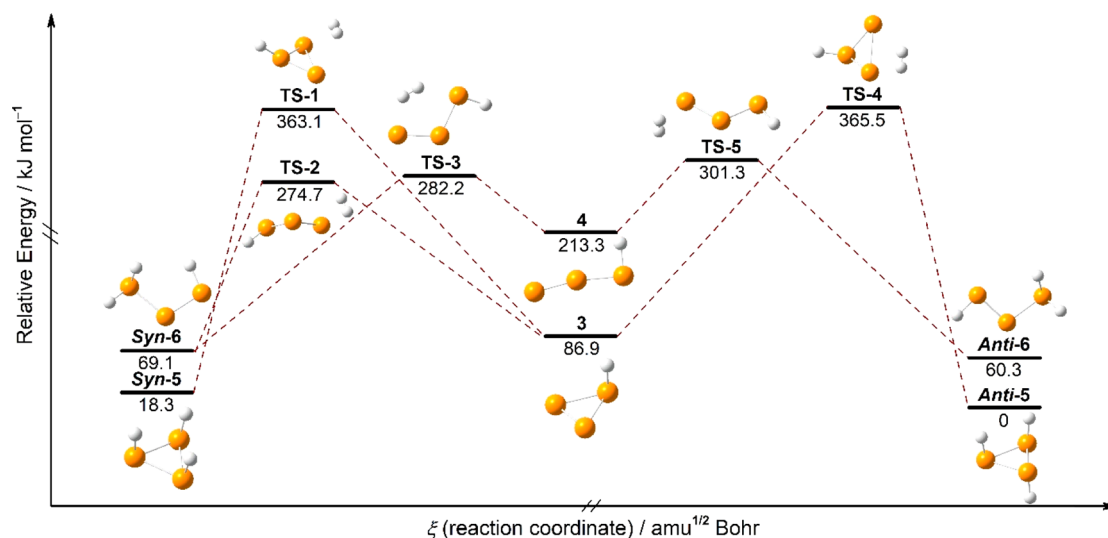
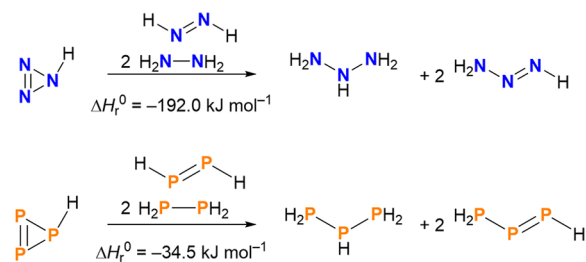


Figure 4. Proposed formation pathways of 1*H*-triphosphirene (*c*-HP₃, **3**) and 2-triphosphenylidene (HP₃, **4**). Energies were obtained at the CCSD(T)/CBS//B3LYP/cc-pVTZ plus zero-point vibrational energies level of theory. Atoms are color coded in white (hydrogen) and orange (phosphorus). Coordinates and normal modes are provided in Tables S7 and S8.

length is computed to be 143.0 pm, longer than the N–N and N–H bond lengths 154.5, 118.5, and 102.6 pm of the 1*H*-triazirine. The longer P–P bonds are assigned to single bonds while the shorter P–P bond is assigned to a double bond.³³ The bond angles of ∠P–P–P are 63.4° and 53.2°. The bond angle of ∠H–P–P is 97.8°, smaller than the bond angle ∠H–N–N 102.1° of 1*H*-triazirine which indicates the preference of phosphorus for a stronger pyramidalization due to a favorable orbital energy splitting, i.e., an energetically low σ_{out} orbital, as well as more spatially diffuse orbitals. Our calculated strain energy of 1*H*-triphosphirene by using a series of homodesmotic equations at the CBS-QB3 level of theory agree with previously reported results from the literature (Figure 5A).¹⁶ In a hypothetical reaction one molecule of *c*-HP₃ reacts with one molecule of H₂P₂ and two molecules of H₄P₂ to form one molecule of H₃P₃ and two molecules of H₃P₃. As all bond types are retained during the reaction, the absolute value of the reaction enthalpy of $-34.5 \text{ kJ mol}^{-1}$ can be attributed to the strain energy in *c*-HP₃ (Figure 5A). This is significantly lower than the calculated strain energy in 1*H*-triazirine ($192.0 \text{ kJ mol}^{-1}$), which indicates the 1*H*-triazirine has a higher tendency to form an open chain isomer, i.e., hydrazoic acid. The transition state for the isomerization of 1*H*-triphosphirene (*c*-HP₃, **3**) to 2-triphosphenylidene (HP₃, **4**) is $195.6 \text{ kJ mol}^{-1}$ high in energy, while the transition state analogue for the isomerization of hydrazoic acid (HN₃, **1**) to 1*H*-triazirine (*c*-HN₃, **2**) lies at $260.4 \text{ kJ mol}^{-1}$ calculated at CCSD(T)/CBS//B3LYP/cc-pVTZ plus zero-point vibrational energies. The calculated HOMO–LUMO (HOMO: highest occupied molecular orbital; LUMO: lowest unoccupied molecular orbital) energy gap of the frontier orbitals of 1*H*-triphosphirene (*c*-HP₃, **3**) is 3.59 eV and much smaller than in 1*H*-triazirine (*c*-HN₃, **2**) (6.48 eV). The HOMO represents the π -system of the unsaturated heterocycle, while the LUMO represents the π^* -orbitals of the pnictogen–pnictogen double bond (Figure 5B).

To conclude, our work reveals the first preparation and identification of the hitherto elusive 1*H*-triphosphirene (*c*-HP₃, **3**) and 2-triphosphenylidene (HP₃, **4**). These molecules are formed in low-temperature phosphine–dinitrogen ices upon

A: Ring Strain



B: Frontier Orbitals

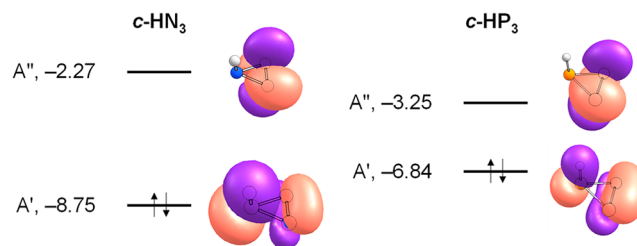


Figure 5. Calculated strain energies (A) and frontier molecular orbitals (B) of *c*-HN₃ (**2**) and *c*-P₃H₃ (**3**). The ring strain energies are calculated via the homodesmotic equations depicted in (A) at the CBS-QB3 level of theory. In a hypothetical reaction one molecule of *c*-HN₃ reacts with one molecule of H₂N₂ and two molecules of H₄N₂ to form one molecule of H₅N₃ and two molecules of H₃N₃. As all bond types are retained during the reaction, the absolute value of the reaction enthalpy of $-192.0 \text{ kJ mol}^{-1}$ can be attributed to the strain energy in *c*-HN₃. The reaction enthalpy for the analogue all-phosphorus equation in (A) is only $-34.5 \text{ kJ mol}^{-1}$. The molecular frontier orbitals in (B) are calculated at the B3LYP/cc-pVTZ level of theory and represent the π - and π^* -systems of the heterocycles. Orbital energies are given in eV. Atoms are color coded in white (hydrogen), blue (nitrogen), and orange (phosphorus).

exposure to energetic electrons at 5 K through decomposition of triphosphirane (*c*-P₃H₃, **5**) and 1-triphosphene (P₃H₃, **6**) transients and were detected isomer selectively exploiting single photon vacuum-ultraviolet (VUV) photoionization coupled with reflectron time-of-flight mass spectrometry (PI-

ReTOF-MS). The enhanced stability of the cyclic 1*H*-triphosphirene (*c*-HP₃, **3**) isomer compared to 2-triphosphirenylidene (HP₃, **4**) is also in line with evolution when substituting second-row atoms by third-row atoms of triatomic molecules carrying group XIV elements. This is best reflected in the (quasi)linear tricarbon molecule (C₃, X¹Σ_g⁺),³⁴ whereas the silicon dicarbide molecule (SiC₂, X¹A₁) is cyclic and partially aromatic.³⁵ Accounting for the distance between the photoionization laser and the ice surface of 2 mm and the average velocity of the isomers subliming in the range 185–215 K of 195 m s⁻¹, the lifetime of the neutral molecules has to exceed 10 ± 1 μs, while the corresponding molecular ions have to “live” for at least 44 ± 1 μs to survive the flight time from the ionization region to the detector of the ReTOF-MS. These discoveries not only transform our fundamental understanding of the electronic structure and chemical bonding of the cyclic, strained main group molecules but also provide an original strategy to “make” highly strained, still obscure molecules such as 1*H*-triazirine (*c*-HN₃, **2**) and tetrahedral tetranitrogen (N₄) in the near future through nonequilibrium chemistries.

■ ASSOCIATED CONTENT

SI Supporting Information

The Supporting Information is available free of charge at <https://pubs.acs.org/doi/10.1021/acs.jpcllett.2c00639>.

Experimental and computational methods details; Figure S1: temperature-programmed desorption (TPD) profile recorded at *m/z* = 94 from the electron processed phosphine (PH₃)-dinitrogen (N₂) and phosphine (PH₃)-15-dinitrogen (¹⁵N₂) ices via photoionization reflectron time-of-flight mass spectrometry (PI-ReTOF-MS) at a photon energy of 10.49 eV; Figure S2: temperature-programmed desorption (TPD) profile of HP₃ at a photo energy of 10.49 eV; Figure S3: molecular structures of P₃H₃ isomers; Table S1: data were used to calculate the average irradiation dose per molecule; Table S2: parameters for the vacuum-ultraviolet light generation used in the present experiments; Table S3: statistical branching ratios for the reaction of the silicon atom with phosphine; Table S3: computed adiabatic ionization energies of distinct HN₃ and HP₃ isomers along with error limits; Table S4: infrared absorption peaks before and after irradiation for phosphine (PH₃)-dinitrogen (N₂)/15-dinitrogen (¹⁵N₂) ices; and Tables S5–S8: Cartesian coordinates, vibrational frequencies, and intensity for selected structures of HN₃, HP₃, P₃H₃, and transition state (TS) structures of P₃H₃ (PDF)

■ AUTHOR INFORMATION

Corresponding Authors

André K. Eckhardt – *Lehrstuhl für Organische Chemie II, Ruhr-Universität Bochum, 44801 Bochum, Germany;*
✉ orcid.org/0000-0003-1029-9272;
Email: Andre.Eckhardt@rub.de

Ralf I. Kaiser – *Department of Chemistry, University of Hawaii at Manoa, Honolulu, Hawaii 96822, United States; W. M. Keck Laboratory in Astrochemistry, University of Hawaii at Manoa, Honolulu, Hawaii 96822, United States;*
✉ orcid.org/0000-0002-7233-7206; Email: ralfk@hawaii.edu

Authors

Chaojiang Zhang – *Department of Chemistry, University of Hawaii at Manoa, Honolulu, Hawaii 96822, United States; W. M. Keck Laboratory in Astrochemistry, University of Hawaii at Manoa, Honolulu, Hawaii 96822, United States*
Cheng Zhu – *Department of Chemistry, University of Hawaii at Manoa, Honolulu, Hawaii 96822, United States; W. M. Keck Laboratory in Astrochemistry, University of Hawaii at Manoa, Honolulu, Hawaii 96822, United States*

Complete contact information is available at:
<https://pubs.acs.org/10.1021/acs.jpcllett.2c00639>

Notes

The authors declare no competing financial interest.

■ ACKNOWLEDGMENTS

This work was supported by the US National Science Foundation (NSF) under Grant AST 1800975 to The University of Hawaii (C.Z., C.Z., R.I.K.). A.K.E. acknowledges the Alexander von Humboldt-Foundation for a Feodor Lynen Return Fellowship.

■ REFERENCES

- (1) Curtius, T. Ueber Stickstoffwasserstoffsäure (azoimid) N₃H. *Berichte der deutschen chemischen Gesellschaft* **1890**, *23* (2), 3023–3033.
- (2) Evers, J.; Göbel, M.; Krumm, B.; Martin, F.; Medvedev, S.; Oehlinger, G.; Steemann, F. X.; Troyan, I.; Klapötke, T. M.; Eremets, M. I. Molecular Structure of Hydrazoic Acid with Hydrogen-bonded Tetramers in Nearly Planar Layers. *J. Am. Chem. Soc.* **2011**, *133* (31), 12100–12105.
- (3) Bräse, S.; Gil, C.; Knepper, K.; Zimmermann, V. Organic Azides: An Exploding Diversity of A Unique Class of Compounds. *Angew. Chem., Int. Ed.* **2005**, *44* (33), 5188–5240.
- (4) Wiss, J.; Fleury, C.; Heuberger, C.; Onken, U.; Glor, M. Explosion and Decomposition Characteristics of Hydrazoic Acid in the Gas Phase. *Org. Process Res. Dev.* **2007**, *11* (6), 1096–1103.
- (5) Furman, D.; Dubnikova, F.; van Duin, A. C. T.; Zeiri, Y.; Kosloff, R. Reactive Force Field for Liquid Hydrazoic Acid with Applications to Detonation Chemistry. *J. Phys. Chem. C* **2016**, *120* (9), 4744–4752.
- (6) Reed, E. J.; Rodriguez, A. W.; Manaa, M. R.; Fried, L. E.; Tarver, C. M. Ultrafast Detonation of Hydrazoic Acid (HN₃). *Phys. Rev. Lett.* **2012**, *109* (3), No. 038301.
- (7) Knyazev, V. D.; Korobeinichev, O. P. Thermal Decomposition of HN₃. *J. Phys. Chem. A* **2010**, *114* (2), 839–846.
- (8) Reed, E. J. Electron-ion Coupling in Shocked Energetic Materials. *J. Phys. Chem. C* **2012**, *116* (3), 2205–2211.
- (9) Pham, C. H.; Lindsey, R. K.; Fried, L. E.; Goldman, N. Calculation of the Detonation State of HN₃ with Quantum Accuracy. *J. Chem. Phys.* **2020**, *153* (22), 224102.
- (10) Evers, J.; Oehlinger, G.; Steemann, F. X.; Klapötke, T. M. Molecular Structure of Hydrazoic Acid from 55 K to Close to the Melting Point Determined with Synchrotron Radiation. *Inorg. Chem.* **2020**, *59* (23), 17671–17677.
- (11) Tang, S. K.; Duo, L. P.; Jin, Y. Q.; Yu, H. J.; Wang, J.; Sang, F. T. Study on HN₃ Production for All Gas-phase Iodine Laser. *Proc. SPIE* **2006**, 6346, L3463–L3463.
- (12) Zhang, J.; Zhang, P.; Chen, Y.; Yuan, K.; Harich, S. A.; Wang, X.; Wang, Z.; Yang, X.; Morokuma, K.; Wodtke, A. M. An Experimental and Theoretical Study of Ring Closing Dynamics in HN₃. *Phys. Chem. Chem. Phys.* **2006**, *8* (14), 1690–1696.
- (13) Yuan, K.; Cheng, Y.; Wang, F.; Yang, X. Photodissociation Dynamics of HN₃ and DN₃ at 157 nm. *J. Phys. Chem. A* **2008**, *112* (24), 5332–5337.

- (14) Phelan, K. G.; Stedman, G. Nitrogen Tracer Evidence for A Cyclic Azide Species. *J. C. S. Chem. Comm.* **1981**, 6 (6), 299–300.
- (15) Calfa, J. P.; Phelan, K. G.; Bonner, F. T. Cyclic Azide As An Aqueous Solution Intermediate: Evidence Pro and Con. *Inorg. Chem.* **1982**, 21 (2), 521–524.
- (16) Glukhovtsev, M. N.; Bach, R. D.; Laiter, S. High-level Computational Study on the Thermochemistry of Saturated and Unsaturated Three- and Four-membered Nitrogen and Phosphorus Rings. *Int. J. Quantum Chem.* **1997**, 62 (4), 373–384.
- (17) Cho, J.-E.; Lee, H.-S.; Choi, C. Structural Isomers and Excited States of HN_3 . *Bull. Korean Chem. Soc.* **2011**, 32, 3641–3643.
- (18) Karahodza, A.; Knaus, K. J.; Ball, D. W. Cyclic Triamines as Potential High Energy Materials. Thermochemical Properties of Triaziridine and Triazirine. *Comput. Theor. Chem.* **2005**, 732 (1–3), 47–53.
- (19) Langmuir, I. The Arrangement of Electrons In Atoms and Molecules. *J. Am. Chem. Soc.* **1919**, 41 (6), 868–934.
- (20) Schoeller, W. W. Small Ring Cyclophosphenes: A Theoretical Evaluation of Bonding Properties. *J. Mol. Struct. (Theochem.)* **1993**, 284, 61–66.
- (21) Bews, J. R.; Glidewell, C. Molecular Fragmentations: Part XIII. The Structures and Energies of Mass Spectral Fragments Derived from Phosphine-3, Diphosphine-4, Diphosphine-2, and Triphosphine-5. *J. Mol. Struct. (Theochem.)* **1983**, 94 (3), 305–318.
- (22) Budnikova, Y. H.; Kafiyatullina, A. G.; Balueva, A. S.; Kuznetsov, R. M.; Morozov, V. I.; Sinyashin, O. G. Transformation of White Phosphorus in the Coordination Sphere of Nickel Complexes with σ -donating Ligands. *Russ. Chem. Bull., Int. Ed.* **2003**, 52 (11), 2419–2423.
- (23) Budnikova, Y. G.; Tazeev, D. I.; Kafiyatullina, A. G.; Yakhvarov, D. G.; Morozov, V. I.; Gusarova, N. K.; Trofimov, B. A.; Sinyashin, O. G. Activation of White Phosphorus in the Coordination Sphere of Nickel Complexes with σ -donor Ligands. *Russ. Chem. Bull., Int. Ed.* **2005**, 54 (4), 942–947.
- (24) Turner, A. M.; Abplanalp, M. J.; Chen, S. Y.; Chen, Y. T.; Chang, A. H.; Kaiser, R. I. A Photoionization Mass Spectroscopic Study on the Formation of Phosphanes in Low Temperature Phosphine Ices. *Phys. Chem. Chem. Phys.* **2015**, 17 (41), 27281–27291.
- (25) Socrates, G. *Infrared and Raman Characteristic Group Frequencies: Tables and Charts*, 3rd ed.; John Wiley & Sons: Hoboken, NJ, 2004.
- (26) Abplanalp, M. J.; Förstel, M.; Kaiser, R. I. Exploiting Single Photon Vacuum Ultraviolet Photoionization to Unravel the Synthesis of Complex Organic Molecules in Interstellar Ices. *Chem. Phys. Lett.* **2016**, 644, 79–98.
- (27) Turner, A. M.; Kaiser, R. I. Exploiting Photoionization Reflectron Time-of-light Mass Spectrometry to Explore Molecular Mass Growth Processes to Complex Organic Molecules in Interstellar and Solar System Ice Analogs. *Acc. Chem. Res.* **2020**, 53 (12), 2791–2805.
- (28) Jones, B. M.; Kaiser, R. I. Application of Reflectron Time-of-flight Mass Spectroscopy in the Analysis of Astrophysically Relevant Ices Exposed to Ionization Radiation: Methane (CH_4) and D_4 -methane (CD_4) as a Case Study. *J. Phys. Chem. Lett.* **2013**, 4 (11), 1965–1971.
- (29) Yu, T.; Peng, H. Quantification and Deconvolution of Asymmetric LC-MS Peaks Using the Bi-Gaussian Mixture Model and Statistical Model Selection. *BMC Bioinf.* **2010**, 11 (1), 559.
- (30) Kuzema, P. O.; Stavinskaya, O. N.; Laguta, I. V.; Kazakova, O. A. Thermogravimetric Study of Water Affinity of Gelatin Materials. *J. Therm. Anal. Calorim.* **2015**, 122 (3), 1231–1237.
- (31) Chernyak, S. A.; Ivanov, A. S.; Strokova, N. E.; Maslakov, K. I.; Savilov, S. V.; Lunin, V. V. Mechanism of Thermal Defunctionalization of Oxidized Carbon Nanotubes. *J. Phys. Chem. C* **2016**, 120 (31), 17465–17474.
- (32) Zheng, W.; Jewitt, D.; Osamura, Y.; Kaiser, R. I. Formation of Nitrogen and Hydrogen-bearing Molecules in Solid Ammonia and Implications for Solar System and Interstellar Ices. *Astrophys. J.* **2008**, 674 (2), 1242–1250.
- (33) Pyykkö, P. Additive Covalent Radii for Single-, Double-, and Triple-bonded Molecules and Tetrahedrally Bonded Crystals: A Summary. *J. Phys. Chem. A* **2015**, 119 (11), 2326–2337.
- (34) Mebel, A. M.; Kaiser, R. I. An *ab initio* Study on the Formation of Interstellar Tricarbon Isomers $\text{l-C}_3(X^1\Sigma_g^+)$ and $\text{c-C}_3(X^3A_2')$. *Chem. Phys. Lett.* **2002**, 360 (1), 139–143.
- (35) Kaiser, R. I.; Krishtal, S. P.; Mebel, A. M.; Kostko, O.; Ahmed, M. An Experimental and Theoretical Study of the Ionization Energies of SiC_2H_x ($x = 0, 1, 2$) Isomers. *Astrophys. J.* **2012**, 761 (2), 178–185.